Mixing of a Shallow Submerged Heated Water Jet with an Ambient Reservoir

BAL M. MAHAJAN* AND JAMES E. A. JOHN†
University of Maryland, College Park, Md.

In order to design an electric powerplant condenser cooling system to minimize thermal pollution, the engineer should have available data concerning the shape of the thermal plume as a function of hot-water exhaust flow and other environmental variables. Unfortunately, such data are not currently available. The work reported here is an attempt to provide information on one aspect of this problem, namely, on the discharge of submerged, turbulent two-dimensional hot-water jets near a reservoir surface. Experimental tests were conducted in a tank 8 ft long, 6 in. wide, 4 ft deep with jet velocities of 8 fps and jet temperatures of 0°, 50°, and 60°C above the tank temperature. For a shallow jet, the effect of the free surface was to cause the jet to move upward, irrespective of temperature difference between jet and reservoir. Flow visualization indicated that this effect was due to a vortex flow generated above the jet. Empirical correlations were obtained which yielded the locus of the point of maximum jet velocity as the jet moved toward the surface. Below the point of maximum velocity, velocity and temperature distributions were similar to those of a deeply submerged jet; above, however, temperatures were considerably higher than those of a deeply submerged jet.

Nomenclature

b_0 = width of slot opening
D = submergence of jet below free surface
g = acceleration due to gravity
U_j = initial velocity of jet
U = x component of velocity
σ, c = empirical constants
β = thermal expansion coefficient
θ = temperature parameter $(T - T_\infty)$
ϵ_m = turbulent kinematic viscosity
ϵ_t = turbulent thermal diffusivity

Subscripts

j = jet properties at exit
m = maximum value across jet cross section
∞ = property of surroundings

Introduction

THERMAL pollution refers to deleterious effects incurred by raising the temperature of a natural body of water above its normal level. In the design and operation of an electric powerplant condenser cooling system that utilizes a large natural body of water for waste heat disposal, the engineer should have available some means to predict the temperatures and flow patterns incurred by the discharge of the warm water. With this information available, he could then proceed to design a system that would, for example, restrict the higher-temperature isotherms to the immediate vicinity of the jet exhaust and limit the volume of water subjected to thermal pollution.

It is the purpose of this investigation to study the flow pattern and temperature distribution incurred by the discharge of a submerged two-dimensional turbulent hot-water jet into a large still reservoir of cooler water. In particular, it is desired to study the effect of the free surface on the resultant flow to determine if, for example, a discharge near the surface could be used to provide a thin layer of hotter water at the surface and increase the evaporative heat loss from the surface of the water to surrounding air. It is recognized that a complete study should include the effects of winds, local reservoir currents, bottom surface contour effects, and three-dimensional effects; however, it was found that the relatively simple case studied here, in which the effect of a limited number of variables was investigated, yielded important and significant information on the flow characteristics of shallow submerged jets.

Presented as Paper 71-17 at the AIAA 9th Aerospace Sciences Meeting, New York, January 25-27, 1971; submitted January 25, 1971; revision received June 16, 1971. This research was partially supported by Water Resources Research Center with funding from Office of Water Resources Research, Department of Interior.

Index category: Jets, Wakes, and Viscid-Inviscid Flow Interactions.

* Instructor. Member AIAA.

† Professor; currently Chairman Department of Mechanical Engineering, University of Toledo. Associate Fellow AIAA.

Analysis

When a fluid jet is discharged into a reservoir of the same fluid, the emerging jet entrains some of the surrounding fluid that was originally at rest. Because of the friction developed on its periphery, the jet spreads outward in the downstream direction while its centerline velocity decreases in the same direction. In other words, in the act of mixing, the jet spreads outward and decelerates in the downstream direction while the surrounding fluid is accelerated or entrained in the same direction. In the case of a deeply submerged jet, the spreading of the jet is symmetrical about its axis or axis of the nozzle.

The case of the discharge of a deeply submerged two-dimensional jet into an infinite reservoir has been studied extensively in the past. The well-established solutions for plane two-dimensional turbulent jets are given below:

$$U_m/U_j = (c/U_j)x^{-1/2} \tag{1}$$

$$U/U_m = \operatorname{sech}^2[\sigma(y/x)] \tag{2}$$

For this solution, the temperature distribution is given by

$$\theta/\theta_m = (U/U_m)^{\epsilon_m/\epsilon_t} \tag{3}$$

In the foregoing, U_m and T_m are the maximum values of velocity and temperature at a jet cross section and, for the deeply submerged case, occur at the geometric centerline of the slot. In the preceding solution, density variations

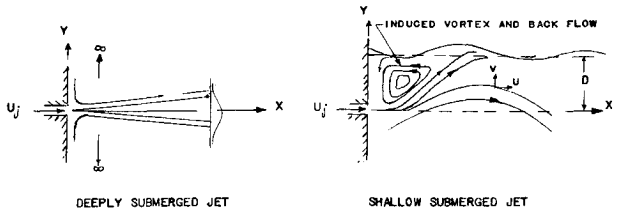

Fig. 1 Jet flow patterns.

due to temperature differences between the jet and surrounding fluid have been neglected.

In the case of a shallow submerged two-dimensional jet, only the lower half of the jet has an infinite supply of water available for entrainment, whereas the supply of surrounding fluid to the upper portion of the jet is limited by the presence of an air-water interface, the free surface. Therefore, the surrounding fluid undergoing induced motion (or being entrained) must be replenished by a back flow both at and near the free surface.

The point at which maximum boil occurs is a critical point, as prior to this point (in the surrounding fluid) the flow at and near the free surface is in the upstream direction (back flow), whereas beyond this point the flow (the jet) is in the downstream direction. This means that some of the fluid is trapped in a region bounded by the wall containing the slot, the free surface, and the upper periphery of the jet. This will set up vortices in the surrounding fluid. Because of the back flow and the vortices set up in the region, the pressure will be considerably lower above the jet than below the jet, and, hence, as a result, there will be a net lift force that will cause the jet to deflect (as a whole) toward the free surface (Fig. 1).

For the shallow jet, the simplifications leading to the use of the boundary-layer equations in the derivation of (1) are not applicable. Moreover, the nonlinear boundary conditions at the free surface make it extremely difficult to obtain analytical solutions to the problem.

For this reason, it was necessary to rely on experimental data for the generation of empirical expressions for velocities and temperatures. The local velocity U in the x direction is a function of $\epsilon_m, U_j, b_0, D, xy, \theta, \rho, \beta, g$. Arranging in dimensionless parameters, there result

$$\frac{U}{U_j} = f_1\left(\frac{x}{b_0}, \frac{y}{x}, \frac{D}{b_0}, \frac{U_j^2}{gb_0}, \frac{\beta\theta g b_0}{U_j^2}\right) \tag{4}$$

$$\frac{\theta}{\theta_j} = f_2\left(\frac{x}{b_0}, \frac{y}{x}, \frac{D}{b_0}, \frac{U_j b_0}{g b_0}, \frac{\epsilon_t}{\epsilon_m}\right) \tag{5}$$

It was assumed that Reynolds number would have only a small effect on turbulent jet flow properties.

Based on the dimensional analysis, the test program was divided into the following parts: 1) to observe visually the effects of submergence on the flow patterns of a shallow submerged two-dimensional jet and the effects of buoyancy in case of heated water jet efflux; and 2) to measure velocity distributions for various shallow submerged jets both with room temperature and heated-water jet efflux and to measure temperature distributions for the two-dimensional heated-water jets.

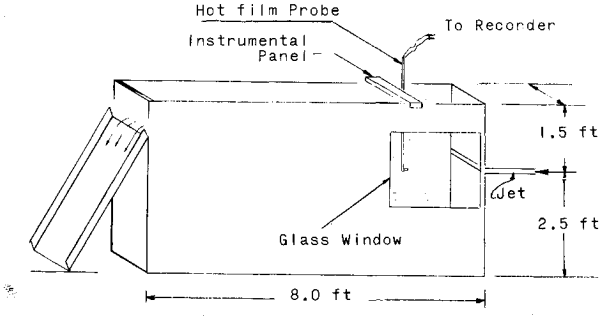

Fig. 2 Apparatus.

Fig. 3 Jet discharge for $D/b_0 = 16$ with $U_j = 8$ fps, $\theta_j = 0$ (jet flow right to left).

Experimental Procedures

The apparatus used in the experiments is shown schematically in Fig. 2; an 8-ft-long, 6-in.-wide, and 4-ft-deep tank made of $\frac{3}{4}$-in.-thick marine plywood was used as the test reservoir. One end of the tank accommodated a $\frac{1}{8}$-in. slot opening 6 in. wide (same as the test tank width), with its centerline 30 in. above the bottom of the tank. The other end of the tank could be closed to any desired height, allowing the reservoir to be filled to any level with water, thus providing the desired submergence of the slot opening below the free surface of water. This also gave an overflow of water, when the jet was being discharged, keeping the water level constant in the tank.

One sidewall of the tank was provided with a 15- × 15-in. glass window for visual observations of the jet. The top of the tank was open, with the upper edges made as smooth as possible, to allow free sliding of a rectangular panel carrying instruments for measuring velocities and temperatures.

A dye was introduced into the jet to allow visual observation and photographs of the flow patterns of the jet discharge. Still pictures were taken using a 35-mm camera.

Because of the low velocities involved, ranging from 0–8 fps, a hot-film anemometer was used to measure the velocities. The hot-film probe support was mounted in the instrument panel, which was placed on the top of the experimental tank and could be moved freely in the horizontal direction. The probe support carrying the hot film could slide in the vertical direction so that the hot-film probe could be placed at any desired position in the flowfield. The vertical distance of the hot-film probe from the centerline of the slot was carefully adjusted and velocity measured at that point. Then the instrument panel carrying the hot-film probe was moved manually in the downstream direction (keeping the probe at a fixed vertical distance), to measure velocities at various

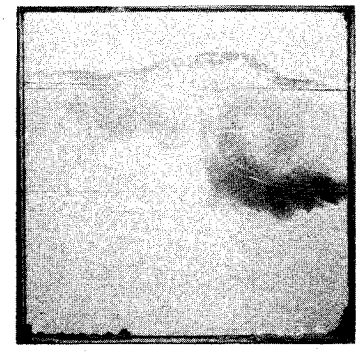

Fig. 4 Jet discharge for $D/b_0 = 32$ with $U_j = 8$ fps, $\theta_j = 0$.

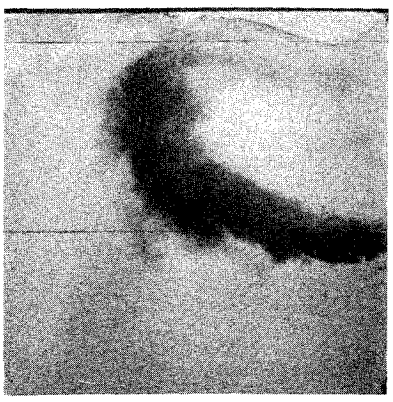

Fig. 5 Jet discharge for $D/b_0 = 48$ with $U_j = 8$ fps, $\theta_j = 0$.

axial distances in the flowfield at constant vertical distance from the slot axis.

A rake of 10 copper-constantan thermocouples was used to measure water temperature for the case of hot-jet efflux. The thermocouples were placed in 1.5-in.-long, $\frac{1}{8}$-in.-diam brass tubes, exposing the tip of the thermocouple at one end of the brass tube. Brass tubes containing thermocouples were soldered to $\frac{3}{32}$-in.-diam steel rod exactly 1 in. apart with all thermocouple tips pointing in the same direction. The output of each thermocouple was read out on a recording potentiometer.

Results and Discussion

1. Visual Observations and Photographs

Typical photographs of the jet discharge are presented in Figs. 3–5, 6a, 7a, and 8a for D/b_0 16, 32, 48, 72, 96, 120 with $U = 8$ fps and $\theta_j = 0$ and in Figs. 6b, 7b, and 8b at D/b_0 72, 96, 120 with $U_j = 8$ fps and $\theta_j = 50°$C.

It is observed from the photographs that the shallow submerged jet deflects toward the free surface regardless of the temperature difference between the emerging jet and the surrounding fluid (that is, whether $T_j - T_\infty = 0$, 50°, or 60°C).

The deflection is affected by the submergence of the jet beneath the free surface. The distance from the origin (the jet opening) at which the upward deflection "apparently" starts depends on the submergence of the jet. The distance, in the downstream direction from the origin, at which the jet axis apparently intersects the free surface also depends on the submergence of the jet.

Examination of Figs. 3–5 shows that the amplitude of the waves created at the free surface is different for each case; the smaller the submergence, the larger the amplitude of the wave formed at the free surface. (This was observed for the other cases also, but the free surface is not visible in the photographs for other submergence.) There were no waves

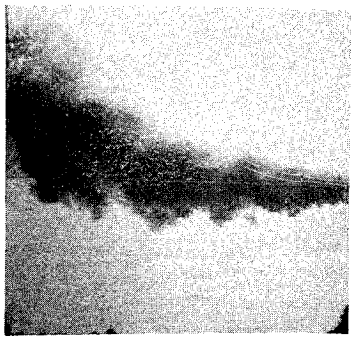

Fig. 7a Jet discharge for $D/b_0 = 96$ with $U_j = 8$ fps, $\theta_j = 0$.

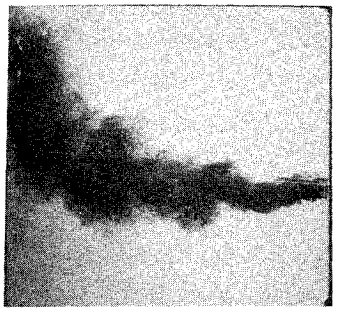

Fig. 7b Jet discharge for $D/b_0 = 96$ with $U_j = 8$ fps, $\theta_j = 50°$C.

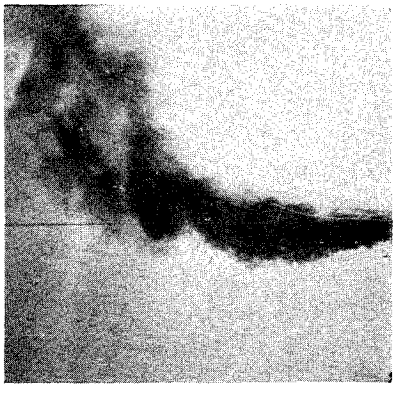

Fig. 6a Jet discharge for $D/b_0 = 72$ with $U_j = 8$ fps, $\theta_j = 0$.

Fig. 6b Jet discharge for $D/b_0 = 72$ with $U_j = 8$ fps, $\theta_j = 50°$C.

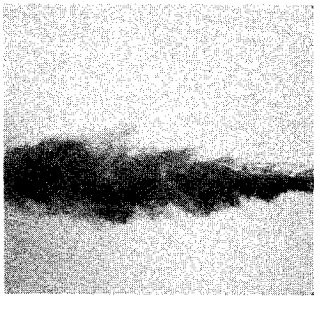

Fig. 8a Jet discharge for $D/b_0 = 120$ with $U_j = 8$ fps, $\theta_j = 0$.

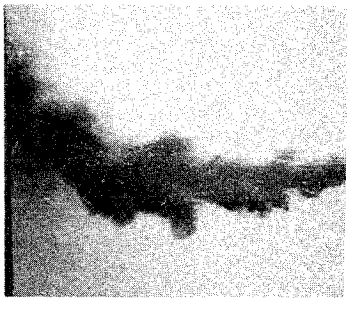

Fig. 8b Jet discharge for $D/b_0 = 120$ with U_j 8 fps, $\theta_j = 50°$C.

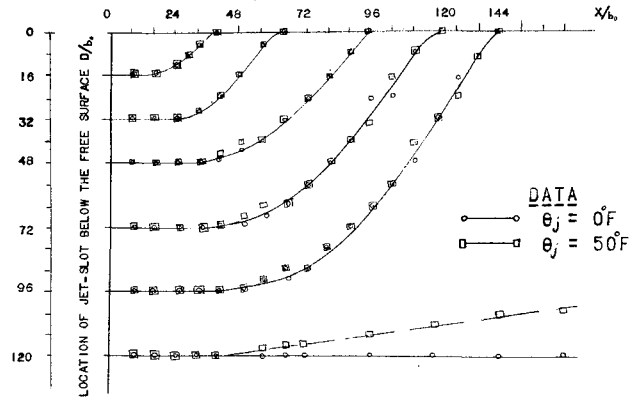

Fig. 9 Loci of points of maximum velocity.

formed at the free surface for $D/b_0 = 120$, which therefore corresponds to a deeply submerged jet; no deflection was observed in this case for $\theta = 0$ (Fig. 8a).

It was observed that, at short distances from the jet opening (origin), vortices were set up in the surrounding fluid on both sides of the jet's periphery and that the strength of the vortex above the jet boundary was much greater than that below the jet boundary. The vortex below the jet periphery was some distance downstream from the vortex above the jet periphery Some fluid from the jet changed direction and became part of the back flow near the free surface; some of the fluid was trapped between the upper periphery of the jet and the free surface Unfortunately, these observations could not be seen in all of the photographs, but a close examination of Figs. 3 and 4 reveals some aspects of these observations.

A comparison of Figs. 6a and 6b, 7a and 7b, and 8a and 8b shows that the jet exit temperature has no visually observable effects on the jet flow patterns (as far as the deflection of the jet is concerned) for the shallow submerged jet. On the other hand, the deeply submerged jet is affected significantly by the buoyancy force, for the hot-water jet discharge.

2. Velocity Distribution

Figure 9 represents the loci of points of maximum velocity at each cross section in the downstream direction. The maximum velocity in a deeply submerged unheated jet is always at the centerline of the jet or at the geometric centerline of the slot. In other words, the physical centerline of the jet (locus of maximum velocity) and the geometric centerline of the slot opening coincide in a deeply submerged jet. However, in the case of a shallow submerged unheated or heated jet, the locus of maximum velocity moves toward the free surface and eventually reaches the free surface.

Referring to Fig. 10, the distance from the origin at which the locus of maximum velocity points apparently starts to move toward the free surface (or the distance at which the jet axis starts to deflect toward the free surface) is called X_1; the distance, in the downstream direction from the origin, at which the jet axis (or the locus of maximum velocity points) apparently reaches the free surface is called X_2. Then the distances X_1 and X_2 are given by the following dimensionless equations, obtained from the experimental data:

$$X_1/b_0 = 1.8(D/b_0)^{0.74} \tag{6}$$

and

$$(X_2 - X_1)/b_0 = 2.85(D/b_0)^{0.745} \tag{7}$$

Now, if any point P on the axis of the shallow submerged two-dimensional jet (or deflection path of the jet or locus of maximum velocity filament) has coordinate $P(X,Y)$, then, from the experimental data,

$$\frac{Y/b_0}{D/b_0} = \frac{Y}{D} = \left\{\frac{X - X_1}{X_2 - X_1}\right\}^{1.43} \tag{8}$$

Equation (8) is valid only for $X_1 \leq X \leq X_2$. The region between these two X values can be called the transition zone.

Equations (6) and (7) are valid only for a shallow submerged two-dimensional jet (submergence range $D/b_0 \leq 96$), and Eq. (8), which gives the deflection path of the shallow submerged two-dimensional jet (or the locus of maximum velocity filament), is valid only for $X_1 \leq X \leq X_2$.

Equations (6) and (7) are plotted in Fig. 11, along with the data points obtained, by extrapolation, from Fig. 9. Equation (8) is plotted in Fig. 12, along with the experimental data.

The typical development of velocity profiles U/U_m (where U_m is the maximum velocity across the jet at any axial distance) vs dimensionless vertical distance Y/b_0 at various axial distances in the downstream direction is presented in Fig. 13 for shallow submerged two-dimensional jets ($D/b_0 = 48$). On these figures are also plotted the existing analytical velocity profiles for the deeply submerged jet, such that $U/U_m = 1$ coincides with the experimental plot (that is, the deflection of the jet is taken into account by vertical shifting of the X axis according to the deflection curve shown in Fig. 10).

An examination of data presented in Figs. 11–13 suggests that the flowfield of a shallow submerged jet can be divided into the following distinct zones:

Zone 1) In this zone, the potential core decays with the spread of the mixing region across the jet. The maximum

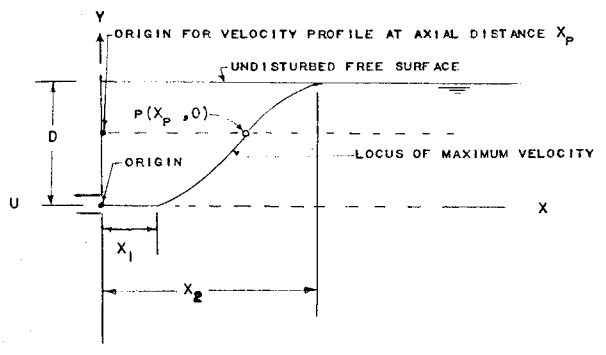

Fig. 10 Path of maximum velocity filament.

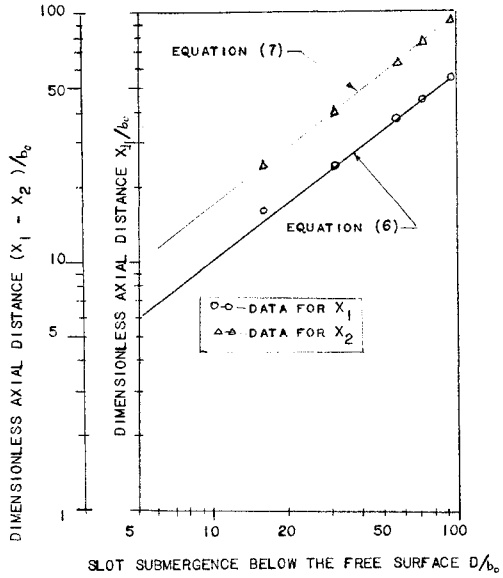

Fig. 11 Equations (6) and (7): comparison with data.

velocity stays at the geometric centerline of the jet (slot). The experimental data for the shallow submerged jets follow closely the analytical velocity profile [Eq. (1)] for a deeply submerged jet. The extent of this zone is from the origin to X_1, with X_1 given by (6).

Zone 2) This is the transition zone, in which the maximum velocity filament starts to migrate toward the free surface and eventually reaches the free surface. This region lies between X_1 and X_2 ($X_1 \leq X \leq X_2$) and is given by Eq. (7). The length of this region increases with an increase in jet submergence. The data agree quite well with existing analytical velocity profiles [Eq. (1)] for a deeply submerged jet in the region below the point of maximum velocity of the shallow submerged jet (i.e., the lower half of the velocity profile). In the upper half of the jet, the experimental velocities (data) are larger than those of deeply submerged jet owing to the influence of the vortex, the backflow at and near the free surface, and the wave disturbance at the free surface.

Zone 3) In this zone, the maximum velocity filament has reached the free surface. This zone can be subdivided into two zones as follows.

Zone 3A) This is the first part of zone 3, immediately downstream from the point at which the maximum velocity filament reaches the free surface. In this region, the velocities near the free surface are still strongly affected by the vortex and wave disturbance formed at the free surface. The data for shallow submerged jets differ from the analytical velocities (lower half of velocity profile) given by Eq. (1) for the deeply submerged jet but follow the same general trend. The extent of this zone again depends on the submergence of the jet.

Zone 3B) In this zone, the wave disturbance at the free surface and vortex have little or no influence on the flow patterns. The data for shallow submerged jets are in close agreement with Eq. (1), actually the lower half of velocity profile for a deeply submerged jet. This part of the flowfield could be considered to be a fully developed shallow submerged jet.

Figure 14 shows the decay of maximum velocity in the downstream direction for the shallow jet along with the decay of maximum velocity in a deeply submerged jet [Eq. (2)]. It is observed that the data start to deviate from the deeply submerged jet relationship at approximately 100 b_0 to 220 b_0 downstream from the origin, depending on the submergence of the jet.

The buoyancy effects are negligible in the shallow submerged jet and yet have a significant effect on a deeply submerged jet. The deeply submerged heated water jet deflected toward the free surface, with a small slope (Fig. 9). The velocity distribution is the same, if the deflection is accounted for, as that for a nonheated deeply submerged jet.

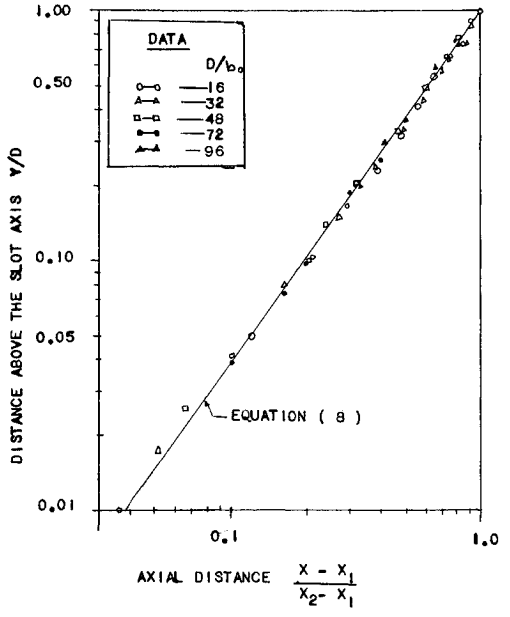

Fig. 12 Equation (8): comparison with data.

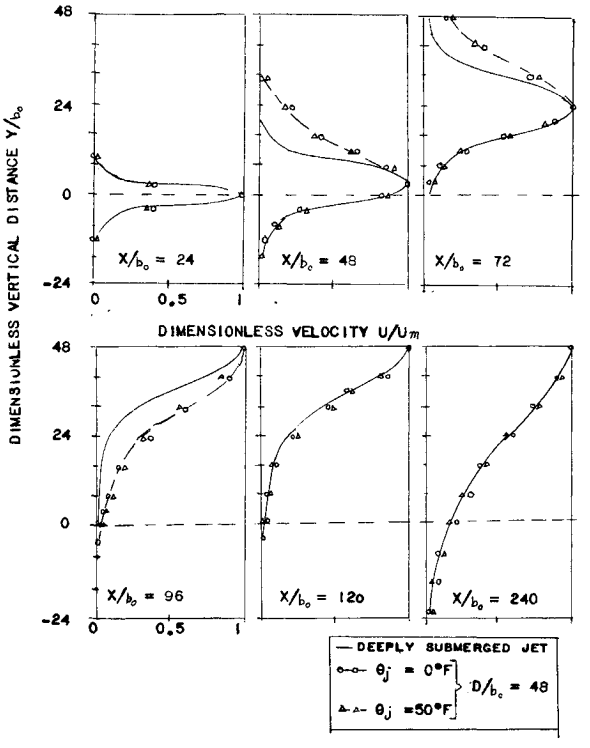

Fig. 13 Development of velocity profile.

3. Temperature Distribution

It is observed from the data, typical results in Figs. 15 and 16, that temperature profiles in a shallow submerged jet deviate from the existing analytical temperature distribution (3) in the first three zones of the jet flowfield. In zone 1 and zone 2, the lower half of the temperature profile has a trend similar to that of a deeply submerged jet, that is, they follow the general equation (3), namely, $\theta/\theta_m = (U/U_m)^{\epsilon_m/\epsilon}$ whereas the upper half is entirely different. As the jet deflects toward the free surface, some of the "jet fluid" becomes part of the backflow and is trapped between the jet periphery and the free surface, causing an increase in the temperature in the upper part of the reservoir above the slot axis. At larger distances in the downstream direction (zone 3B), the temperature profile closely follows Eq. (3), whereas in zone 3A it also follows (3).

In Eq. (3), ϵ_m/ϵ_t is the turbulent Prandtl number and is not constant for the entire flowfield but actually depends on the turbulence level in the flowfield, which in turn depends on the local velocities. Reichardt's[1] experimental result,

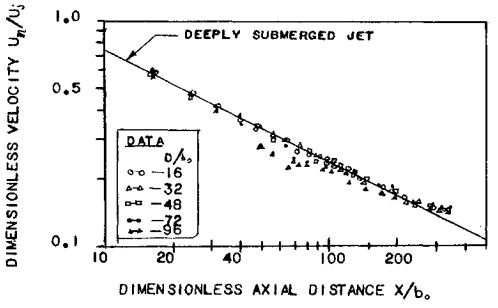

Fig. 14 Decay of maximum velocity in the downstream direction.

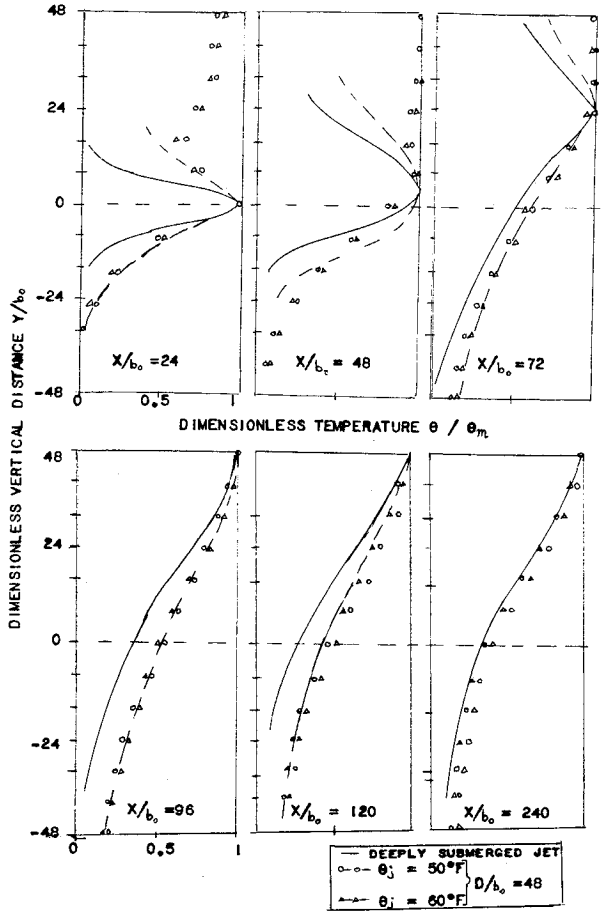

Fig. 15 Development of temperature profile.

performed with heated air jets, indicated that $\epsilon_m/\epsilon_t = \frac{1}{2}$ gave good agreement with experimental results. For the case under investigation here, it was found that values of turbulent Prandtl number $\epsilon_m/\epsilon_t = 0.5$ gave reasonable agreement with the experimental data in zone 1 for the lower half of the temperature profile. Furthermore, $\epsilon_m/\epsilon_t = 0.4$ gave reasonable agreement with the experimental data in the transition zone of a shallow submerged jet (actually for the lower half of temperature profile in zone 2 and for the temperature profile in zone 3A), and $\epsilon_m/\epsilon_t = 0.5$ agreed closely with the experimental data in zone 3B.

Equation (3) is plotted in Fig. 15 (in the transition zone for $\epsilon_m/\epsilon_t = 0.4$, 0.5, and elsewhere for $\epsilon_m/\epsilon_t = 0.5$), along with the data.

It is observed from these figures that the maximum temperature reached the free surface at a shorter distance downstream, from the origin, than maximum velocity.

Hence, the temperature distribution in a shallow submerged two-dimensional jet can be obtained, to a reasonable agreement, except for the upper part of temperature profile in zone 1 and zone 2, using Eq. (3):

$$\frac{\theta}{\theta_m} = \frac{T - T_\infty}{T_m - T_\infty} = \left(\frac{U}{U_m}\right)^{\epsilon_m/\epsilon_t}$$

where (U/U_m) can be obtained for shallow submerged jets as explained previously.

Figure 16 shows a comparison between the decay of maximum temperature in the downstream direction for a deeply submerged jet (existing analytical) and shallow submerged jet at approximately $X/b_0 = 200$ downstream from the origin. The maximum temperatures of the shallow submerged jet (data) are slightly lower than for a deeply submerged jet, because of the heat transfer to the environment from the free surface.

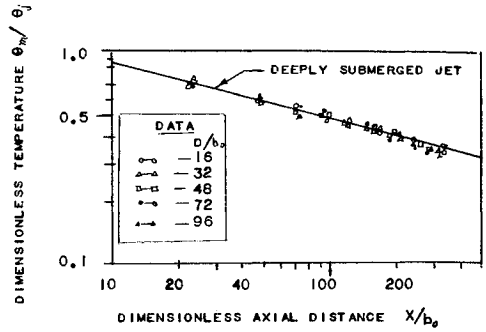

Fig. 16 Decay of maximum temperature in the downstream direction.

Hence, use of a shallow submerged jet will confine the high-temperature water to a small region close to the free surface, thereby allowing the transfer of more heat to the environment. This concept, if incorporated in the design of cooling water discharge systems, may improve over-all efficiency of such a system.

Conclusions

1) The flowfield of a shallow submerged jet can be divided into the following distinct zones:

Zone 1) In this zone, the potential core of the jet decays with an increase in width of the mixing region; the flow patterns are the same as those of a deeply submerged jet.

Zone 2) This is the transition zone. The flow patterns of a shallow submerged jet are quite different from those of a deeply submerged jet in this zone. The maximum velocity line moves toward the free surface as the flow proceeds downstream and eventually reaches the free surface. The extent of zone 1 and zone 2 is a function of the submergence of the jet.

Zone 3) The maximum velocity line has reached the free surface. The flow patterns of a shallow submerged jet, in this zone, are similar to those of the lower half of a deeply submerged jet.

2) The velocity distribution in a shallow submerged jet is quite similar to that of a deeply submerged jet if the deflection of the jet is taken into account, except in zone 2 and the first part of zone 3, where velocities are higher in the regions close to the free surface. If the locus of the maximum velocity filament is considered as the jet axis, the available solution for a deeply submerged jet gives reasonable agreement with the experimental data.

3) The buoyancy, in the case of the heated-water jet (for the two-dimensional case), has negligible effect on the flow patterns of a shallow submerged jet but has significant effects on the flow patterns of a deeply submerged jet.

4) The temperature distribution in a shallow submerged two-dimensional jet follows the same general relationship to the velocity distribution as that in a deeply submerged jet.

5) The flow patterns of a shallow submerged two-dimensional jet can be derived by first obtaining the deflection path of the jet with the aid of empirical equations and then utilizing the velocity profiles from the available solutions for deeply submerged jets.

Reference

[1] Schlichting, H., *Boundary Layer Theory*, McGraw-Hill, New York, 1955.